Expression of Cyclin-Dependent Kinase 6, but not Cyclin-Dependent Kinase 4, Alters Morphology of Cultured Mouse Astrocytes

Karen K. Ericson, David Krull, Peter Slomiany, and Martha J. Grossel

Department of Biology, Connecticut College, New London, CT

Abstract

Disruption of the pRb pathway is a common mechanism in tumor formation. The D-cyclin-associated kinases, cyclin-dependent kinase (cdk) 4 and cdk6, are important regulators of the G_1-S phase transition and are elevated in several types of cancers, including gliomas. To investigate potential functional differences in these kinases, mouse astrocytes were taken from chimeric mice and propagated in tissue culture. These multipolar tissue-culture astrocytes were infected with viruses expressing either cdk4 or cdk6. Interestingly, expression of cdk6 resulted in a distinct and rapid morphology change from multipolar to bipolar. This change was not observed in control astrocytes or in astroyctes infected with cdk4. Several other differences in cdk4- and cdk6-infected cells were noted, including differential binding to a subset of cell-cycle inhibitor proteins and a distinct pattern of subcellular localization of these kinases. Immunoblot and immunofluorescence analyses revealed that cdk6-infected astrocytes had an altered expression profile of known markers of glial differentiation. Together, these data indicate several important differences between cdk4 and cdk6 that highlight unique functional roles for these cyclin-dependent kinases.

Introduction

The G_1 cyclins and associated cyclin-dependent kinases are critical regulators of G_1 phase of the cell cycle. Cell cycle progression is dependent on mitogenic signals that activate cyclin D and its associated kinases. Cyclin-dependent kinase (cdk) 4 and cdk6 partner with cyclin D proteins to phosphorylate the Retinoblastoma protein (pRb), allowing onset of S-phase (for review, see Ref. 1). Since the initial characterization of cdk6, the D-cyclin kinases have been widely thought to act redundantly to regulate the cell cycle through the phosphorylation of pRB (2–5). However, recent studies have uncovered novel functions of cdk6 and several studies highlight differences between cdk4 and cdk6. For instance, cdk6 plays a role in halting inappropriate cellular proliferation through a mechanism involving the accumulation of the p53 and p130 growth-suppressing proteins (6), and activation of cdk6 precedes cdk4 activation in T cells (7, 8). Also, differences in subcellular localization of cdk4 and cdk6 and in the timing of nuclear localization have been noted in several cell types by several researchers (9–12). Data from tumor studies also suggest differences in these kinases. Cdk4, and not cdk6, is specifically targeted in melanoma (13, 14) while cdk6 activity has been found to be elevated in squamous cell carcinomas (15, 16) and neuroblastomas (17) without alteration of cdk4 activity. Cumulatively, these data suggest that cdk4 and cdk6 have unique functions that may be cell-type specific, temporally regulated, or developmentally distinct.

The process of differentiation can be considered as coupled processes including: (*a*) exit from the cell cycle and (*b*) expression of tissue-specific genes (18). Differences in protein levels and activity of key cell cycle inhibitors have been noted on differentiation of some cells. For instance, the cdk inhibitor protein, $p27^{kip1}$, has been identified as part of a timing mechanism that causes oligodendrocyte precursor cells to withdraw from the cell cycle and undergo differentiation. In this system, $p27^{kip1}$ accumulation correlates with differentiation of oliodendrocytes (19–21). Expression of $p21^{CIP1/WAF-1}$, another cyclin kinase inhibitor protein, has been associated with differentiation in a variety of tissues (22–26). In murine erythroleukemia (MEL) cells, inhibitors that blocked both cdk2 and cdk6 induced differentiation, but inhibition of cdk2 and cdk4 did not (24). Thus, G_1 phase inhibitors have been shown to be important in the process of differentiation in muscle, blood, and adipocytes (18).

We set out to study functional differences of cdk4 and cdk6 using a previously described tissue-culture astrocyte model system. This system was chosen because these cells contain a minimal number of genetic mutations and are physiologically relevant, since overexpression of cdk4 and cdk6 has been found in glioblastomas and astrocytomas (27–30). These primary astrocytes were isolated from newborn transgenic mice that had been engineered to express the Avian Leukosis Virus (ALV) receptor (TVA) downstream of the GFAP promoter (G-tva) (31). Only GFAP-producing cells expressed the viral receptor and thus only these cells could be infected with ALV (31, 32). Starting cultures of these astrocytes displayed a star-shaped astrocytic morphology with multiple short projections from a central cell body. Importantly, these cultures did not resemble a bipolar, fibroblast-like morphology typical of glial restricted precursors or type 1 astrocytes [for further descriptions of glial differentiation, see Lee *et al.* (33)]. Because cdk4 expression has been well characterized in this system (32), these tissue culture

Received 1/13/03; revised 4/22/03; accepted 5/7/03.
The costs of publication of this article were defrayed in part by the payment of page charges. This article must therefore be hereby marked advertisement in accordance with 18 U.S.C. Section 1734 solely to indicate this fact.
Grant support: NSF under CAREER grant #9984454 to Martha J. Grossel.
Requests for reprints: Martha J. Grossel, Department of Biology, Box 5331, Connecticut College, 270 Mohegan Ave., New London, CT 06320. Phone: (860) 439-5209; Fax: (860) 439-2519. E-mail: mjgro@conncoll.edu

astrocytes provided an ideal model in which to compare known functions, and to investigate novel functions of cdk4 and cdk6. Results presented here demonstrate that infection of cdk6, but not cdk4, is sufficient to cause morphogenesis of cultured mouse astrocytes.

Results

Morphological Differences in Cdk4- and Cdk6-Infected Astrocytes

To study overlapping and discreet functions of cdk4 and cdk6, G-tva mouse astrocytes were infected with either of the two D-cyclin-associated kinases or alkaline phosphatase (AP) as a control. Astrocytes were infected with viral supernatants from DF-1 cells producing ALV that expressed the cDNAs of AP, cdk4, or cdk6. Protein expression in transfected DF-1 cells was confirmed by immunoblot and virus-containing supernatants from DF-1 cells were filtered onto G-tva mouse astrocytes and infected for 3 days. Protein expression of cdk4 and cdk6 in these astrocytes was confirmed by immunoblot (Fig. 1A). Endogenous cdk6 was not expressed to detectable levels in these astrocytes.

Within days after infection, it was apparent that cdk6-infected astrocytes had a strikingly different morphology than those infected with cdk4. The cdk6-infected cells displayed a fibroblast-like, bipolar morphology. Digital images of these

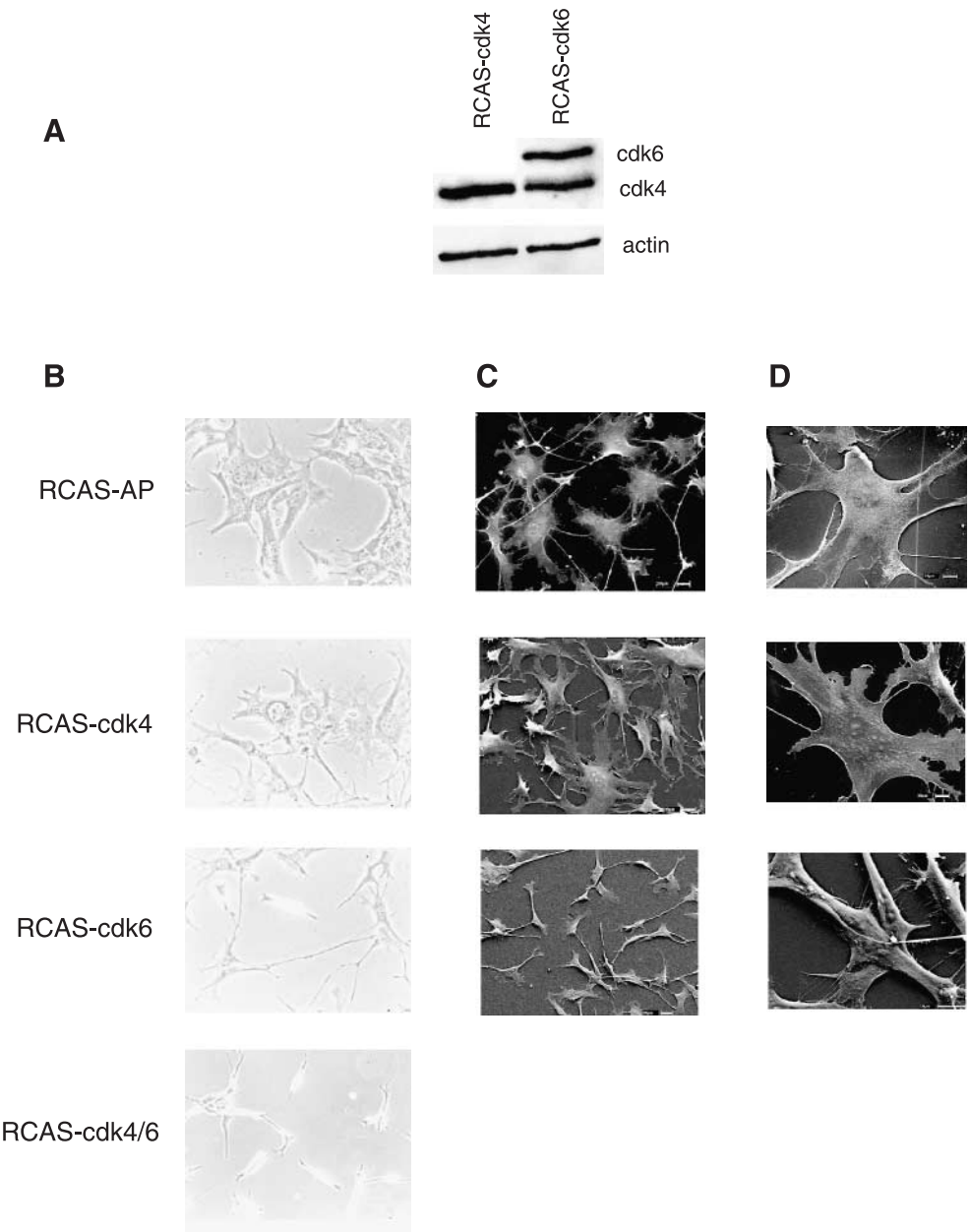

FIGURE 1. Morphology of AP-, cdk4-, and cdk6-infected astroyctes. **A.** Immunoblot of primary mouse astrocytes infected with AP, cdk4, or cdk6, as indicated. One hundred twenty micrograms of protein extract were loaded per lane. The blot is probed with a mixture of cdk4 and cdk6 antibodies to detect both proteins on one blot. **B.** Phase-contrast microscopy of infected astroyctes grown in monolayer. All images are taken at the same magnification. RCAS-cdk4/6 are RCAS-cdk4-infected astrocytes that were super-infected with RCAS-cdk6 virus. **C**, **D.** Scanning electron microscopy (SEM) of fixed astrocytes at lower (**C**) and higher (**D**) magnifications. *Scale bars* on images indicate size. In panel **C**, *scale bar* is 20 μM; in panel **D**, *scale bar* is 10 μM.

cells grown in a monolayer are shown in Fig. 1B. Alkaline-phosphatase and cdk4-infected astrocytes displayed a star-shaped, flat morphology containing several short projections emanating from a wide central cell body. In sharp contrast, cdk6-infected mouse astrocytes displayed an elongated spindle-shaped morphology with bipolar processes. Cdk6-infected cells contain a narrow soma that is collapsed around the nucleus and greatly extended projections emanating from the central cell body. In addition, many of the cells are phase-bright in the area surrounding the central cell body, a property not seen in AP and cdk4 cells. The projections that extended from the cdk6 cells formed connections between adjacent cells and often contained bulbous protrusions. This striking morphology was apparent within days of the start of infection, was prominent in all four independent infections, and persisted in cells carried for several months.

Scanning electron microscopy was used to further investigate the morphology of these ALV-infected mouse astrocytes. Cells were grown in culture to a confluence of 40–60%, fixed, and prepared for scanning electron microscopy. Representative results of these studies are shown in Fig. 1, C and D. The vast majority of AP and cdk4 cells displayed a star-shaped morphology and exhibited several short projections off a central cell body, while cdk6 cells displayed a spindle-shaped morphology with long bipolar projections emanating from a condensed cell body in which the cytoplasm is essentially collapsed against the nucleus. In addition, cdk6-infected cells appeared smaller than their AP- and cdk4-infected counterparts. Higher magnification images confirmed these differences, highlighting the large central cell body of AP-infected and cdk4-infected cells and the associated short, wide, flattened projections. The cdk6 cells displayed filopodia and lamellopodia and contained long fibers that ran across the nucleus and into the bipolar projections. These cells were also notably less flattened than the cdk4 cells. It is important to note that this altered phenotype was present in virtually all cdk6-infected cells. Several indicators determined that cells with this altered morphology are not derived from a subset of cells being selected out from a diverse population of cells. First, in four independent experiments comparing AP, cdk4, and cdk6, only cdk6-infected cells displayed this phenotype and the morphology was consistent in each of four independent infections. Second, the model system used ensures that only GFAP-expressing cells can be infected by the ALV retroviruses expressing cdk6. Immunoblots confirm that cdk6 was expressed and fluorescence indicated that green fluorescent protein (GFP) was produced in these cells. Third, the phenotype appeared rapidly after infection; all cells displayed the altered morphology within 7 to 10 days after infection and the phenotype can be seen as early as the end of the 3-day infection period. Finally, established cdk4-expressing cells with the multipolar, star-shaped morphology were super-infected with RCAScdk6 virus. These super-infected cells, shown in monolayer in Fig. 1B, exhibited the bipolar phenotype typical of cdk6-infected astrocytes. Thus, even in preestablished cdk4-expressing astrocytes, cdk6 induced a morphological change.

The striking morphology differences between the same primary cells expressing cdk4 and those expressing cdk6 clearly indicate that cdk6 has a unique function or functions not shared with cdk4.

Cdk4-Infected and Cdk6-Infected Cells Display Distinct Growth Curves

Changes in cell size associated with cdk6 expression might be a result of changes in cellular proliferation. To study cell division properties of cdk4 and cdk6, growth curves were generated. Infected astrocytes were grown until confluent and then were split, counted, and replated at a density of 1×10^5 cells per plate and followed over a period of up to 120 days. Growth curves of one of four independent infections are displayed in Fig. 2. The growth curves of both cdk4- and cdk6-infected cells were remarkably consistent across all infections; in four separate trials of cdk4 and cdk6 infections, these cells escaped crisis. In contrast, AP-infected cells underwent a more sustained and lasting crisis in all four infections and in two of four infections underwent cell death starting at approximately day 20 and continuing until day 50 when no cells remained on the plate. The remaining two AP infections underwent the sustained crisis, slowed growth at day

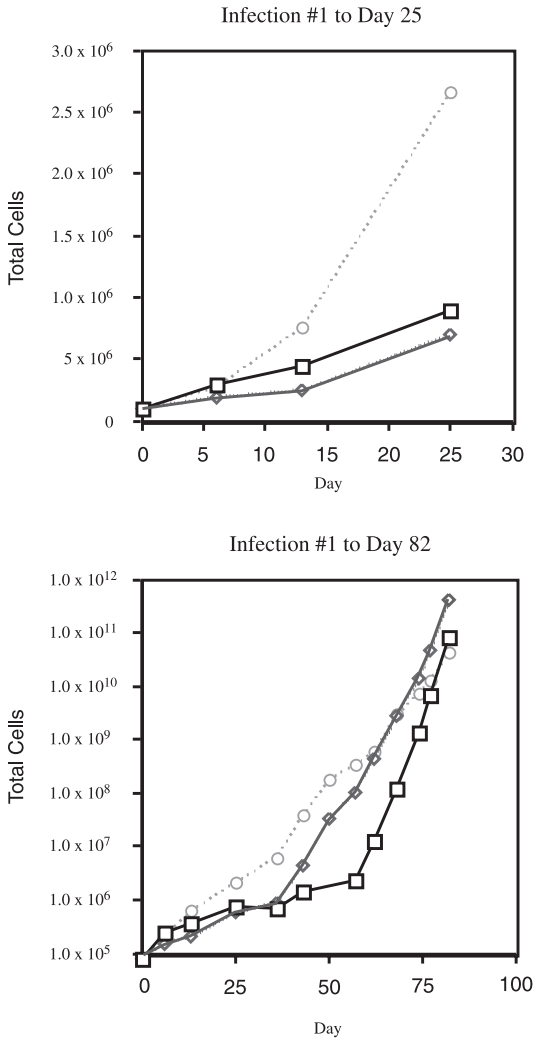

FIGURE 2. Growth patterns of cdk4 and cdk6. Growth curves of primary mouse astrocytes infected with ALV expressing AP, cdk4, or cdk6. These data illustrate consistent differences observed between cdk4- and cdk6-infected astrocytes. Infection #1 is shown at both early (*top panel*) and later (*bottom panel*) stages. AP, —□—; Cdk4, —♦—; Cdk6, ···○···.

20–40, and survived crisis to continue to divide in culture (shown in Fig. 2). Unlike cdk4- and cdk6-infected cells, these cells proliferated for two or three passages and then for the most part ceased division until almost 2 months after the infection—a period during which cdk4- and cdk6-infected cells underwent 10 passages and 8 population doublings. The surviving AP-infected cells (or cell) had likely sustained a mutation, or mutations, that allowed an escape from crisis. The lagging growth curve of AP-infected cells was distinctly separate from the patterns of growth for cdk4- and cdk6-infected cells, which were remarkably consistent in each of the four independent infections. Late in the growth curve of AP-infected cells, the rate of division exceeded that of cdk4- and cdk6-infected cells, further supporting the notion that these cells sustained a mutation that conferred a proliferative advantage to these cells. Cdk6-infected cells displayed a faster rate of division in the first month than did cdk4 cells and later in the time course, the rate of division of cdk4-infected cells surpassed that of cdk6-infected cells. Although there were no large differences in the growth curves of astrocytes expressing cdk4 or cdk6, the curves were reproducibly distinct.

Profiles of Cell Cycle Proteins, pRb Kinase, and Binding Studies

To begin to eludicate the mechanism by which cdk6 expression causes changes in morphology, key cell cycle regulators were studied. To determine if cdk6-dependent changes were due to differences in the levels of key cell cycle proteins, immunoblots were performed using lysates of infected cells. Protein levels of the D-type cyclins and members of the INK family of inhibitors from AP-, cdk4-, and cdk6-infected astrocytes were analyzed and are shown in Fig. 3A. These primary mouse astrocytes expressed detectable levels of all three D-type cyclins. Cyclin D1, D2, and D3 were present at slightly elevated levels in cdk4-infected cells as compared to AP-infected cells while cdk6-infected cells showed intermediate levels of the D cyclins. The INK4a family of inhibitors was also studied. When equivalent amounts of protein extract from AP, cdk4, and cdk6 cells were analyzed, levels of p15 protein were slightly lower in cdk6-infected cells. The p16 protein was detected in cdk6-infected cells only when 800 μg or greater cell extract were assayed and no p16 protein was detected in blots containing 800 μg of AP- or cdk4-infected cell extract. It is possible that cdk6 induces expression of p16 or stabilizes the p16 protein, although clearly not to an extent great enough to cause cell cycle arrest. The p18 protein was barely detectable in cdk6-infected cells and not detected in AP- or cdk4-infected cells (data not shown). Immunoblot analysis of p53 indicated that p53 protein levels were approximately equal in all three infections (Fig. 3B). In addition, each of the three infected astrocytes was able to induce p21 in response to camptothecin-induced DNA damage, indicating that the p53 present in AP-, cdk4-, and cdk6-infected cells was functionally wild-type (Fig. 3C). This figure also allows comparison of p21 protein levels in infected astrocytes. The lanes without camptothecin clearly show that p21 protein is elevated in cdk4-infected cells. This result, reproduced in four independent experiments, may suggest that cdk4 overexpression up-regulates p21 expression or in some way stabilizes the p21 protein.

Previous studies in leukemic cells have shown that induction of cell cycle inhibitors affected cdk4 pRb kinase activity but not

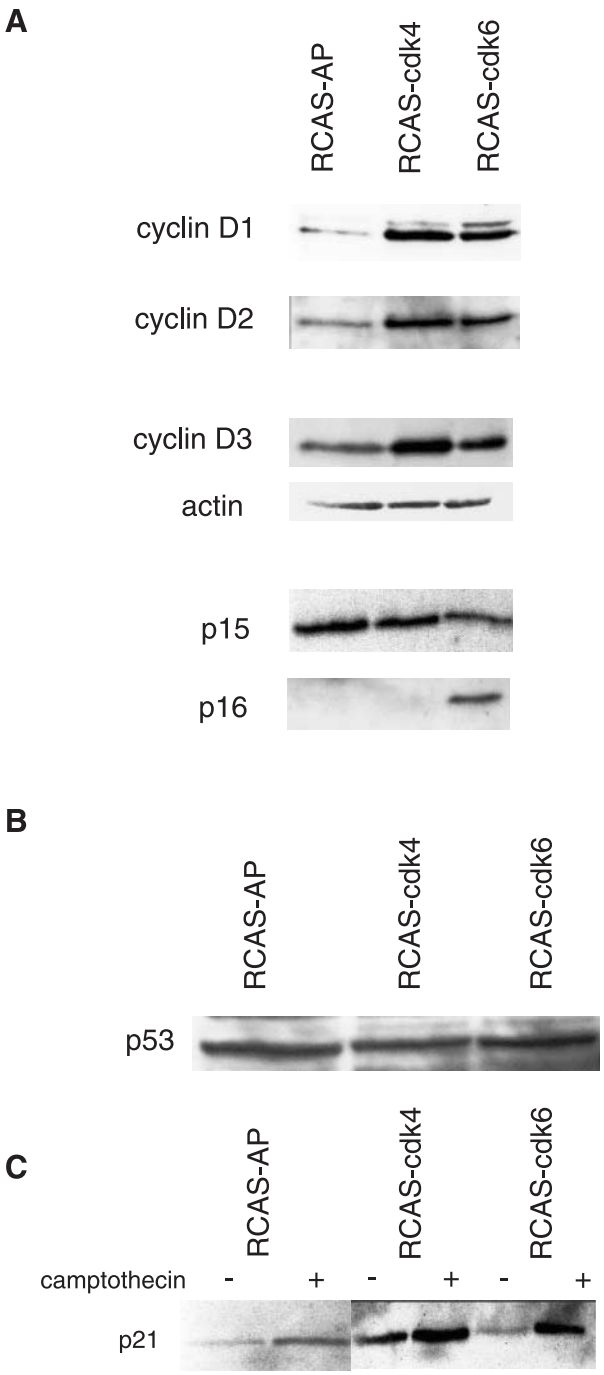

FIGURE 3. Immunoblots of cell cycle regulatory proteins. **A.** Immunoblots of AP-cdk4- and cdk6-infected astrocytes, as noted. Cyclin D1, D2, and D3 contain 150 μg of protein per lane. Inhibitor blots contain the following amounts of cell extract per lane: p15, 100 μg; p16, 150 μg. Actin is blotted as a loading control in all blots shown; actin blot of cyclin D3 is shown as a representative loading control. **B.** p53 immunoblot with 100 μg of protein loaded per lane. **C.** Analysis of p53 status. p21 protein was analyzed by immunoblot of 100 μg cell extract from 27 cells that had been left untreated (−) or had been treated (+) with the DNA-damaging agent, camptothecin. All data are representative of at least two independent experiments.

cdk6 pRb activity (24, 34, 35). These findings prompted us to test if cdk6 bound these inhibitors differently than cdk4 in this system. When the binding of cdk4 and cdk6 to p21 and p27 was examined, clear differences in affinities of the kinases for these inhibitors were noted. When cdk4 or cdk6 were immunoprecipitated and blotted with p21 antibody, p21 was observed to bind strongly to cdk4 and binding to cdk6 was not detected. This preferential cdk4 binding was confirmed in the reciprocal immunoprecipitation where p21 was immunoprecipitated followed by an immunoblot using antibodies to both cdk4 and cdk6 (Fig. 4A). The Cip/Kip inhibitor p27 also bound cdk4 better than it bound cdk6; both when tested via a kinase immunoprecipitation followed by a p27 immunoblot or through a p27 immunoprecipitation followed by a combined cdk4 and cdk6 immunoblot. Importantly, these differences were not simply due to differences in levels of inhibitor protein, since immunoblots of p21 and p27 from these same cell lysates demonstrated that both cdk4- and cdk6-infected cells contain similar amounts of p21 and p27 protein (Fig. 4A). Thus, the binding patterns of p21 and p27 demonstrate a clear distinction between cdk4 and cdk6, one that could play a role in the dedifferentiation function of cdk6.

The ability of cdk4 and cdk6 to phosphorylate pRb *in vitro* was also examined. *In vitro* kinase assays of cdk4- and cdk6-infected cell extracts were performed using the relevant antibodies and a C-terminal pRb protein. Results shown in Fig. 4B show that cdk4-immunoprecipitates from cdk4-infected cells and cdk6-immunoprecipitates from cdk6-infected cells are both able to phosphorylate pRb *in vitro*. In multiple kinase assays, cdk6 immunoprecipitated from cdk6-infected cells demonstrated approximately 50–75% less pRb kinase activity than did cdk4 immunoprecipitated from cdk4-infected cells or from AP-infected cells. A cdk6-immunoprecipitation from AP-infected cells was not performed since there is no measurable endogenous cdk6 protein in these astrocytes. *In vivo* phosphorylation of pRb was determined by immunoblot to detect the presence of hyperphosphorylated Rb (Fig. 4C). These data show that pRb exists in both its hypo- and hyper-phosphorylated forms in asynchronous populations of AP-, cdk4-, and cdk6-infected cells. In cdk6-infected cells, the hypophosphorylated and hyperphosphorylated forms of pRb are approximately equal while in AP- and cdk4-infected cells, hypophosphorylated pRb was slightly more prominent than hyperphosphorylated pRb. The data in Fig. 4 demonstrate that cdk6 binds p21 and p27 less well than cdk4, and cdk6 appears to be a poorer enzyme for *in vitro* pRb phosphorylation. These data highlight differences in these two D-cyclin kinases and indicate that these kinases, often assumed to have redundant functions, may indeed have independent functions.

Cdk6-Infected Astrocytes Express a Varied Profile of Differentiation Markers

The morphology of cdk6-expressing cells is similar to that of glial precursor cells. Glial precursors give rise to astrocytes and oligodendrocytes and have a well-characterized fibroblast-like morphology. To determine the protein levels of a subset of glial-differentiation markers, well-established cultures (60 or more days in culture) of infected astrocytes were characterized. Immunofluorescence and immunoblot studies on infected astrocytes indicated that cells infected with AP, cdk4, or cdk6 were GFAP-positive (Fig. 5A). Indirect immunofluorescence indicated that these infected cells were also A2B5-positive (Fig. 5A). Together with the multipolar phenotype of starting cultures and AP- and cdk4-infected cells, these data suggest that these cells were not type 1 astrocytes. Furthermore, immunofluorescence and immunoblot studies indicated that none of the infected astrocytes expressed O4, a marker for oligodendrocytes and their precursors, nor did they express β-tubulin, a marker for neurons (data not shown).

Interestingly, several immunoblots demonstrated that cdk6-infected astrocytes varied from cdk4- and AP-infected cells in the expression profile of certain protein markers of glial differentiation (Fig. 5B). Protein concentrations of cell extracts were determined and equal amounts of protein from cells infected with AP, cdk4, or cdk6 were compared by immunoblot analysis. Actin protein was immunoblotted to serve as a protein loading control. In these studies, cdk6-infected cells contained higher levels of the protein PLP than did AP-infected or cdk4-infected cells. PLP is myelin proteolipic protein that is expressed in oligodendrocytes and in glial progenitors. Immunoblots also revealed that cdk6-infected cells contained more Id4 protein than either AP- or cdk4-infected astrocytes. Id4, a helix loop helix transcription factor, has been found to be down-regulated on differentiation of glia (36) and retained at high levels in precursor cells (33). Thus, both PLP and Id4 proteins are present at higher levels in glial precursor cells than in differentiated astrocytes. Cdk6-expressing cells also contained slightly less vimentin protein than did cdk4-infected cells. This vimentin blot also provided an excellent internal control for experimental consistency since the same blot probed for PLP (up in cdk6) was stripped and re-probed with vimentin (down in cdk6), ensuring that there was no error in quantitating protein concentrations or in gel loading. Immunoblots of NG2 proteoglycan, a marker to identify O2-A precursor cells, were also performed. No NG2 protein was detected in any of the astrocytes with up to 200 μg of cell extract tested. It remains to be determined if these cells are similar to the well-characterized glial-restricted precursor cells (37). Since differentiated astrocytes possess lower levels of PLP and Id4 than precursor cells, the protein pattern observed in cdk6-infected astrocytes was consistent with that of immature glial cells and distinct from the AP- and cdk4-infected astrocytes. A similar expression pattern of differentiation markers was observed when GFAP-expressing mouse astrocytes were infected with virus expressing platelet-derived growth factor (PDGF). PDGF expression in these cultured astrocytes resulted in changes in morphology and in differentiation markers consistent with that of glial precursors (38). Unlike these astrocytes, cdk6-infected cells did not show an increase in the expression of the PDGF receptor, PDGFRβ, as compared to AP- and cdk4-infected astrocytes. The profile of differentiation markers and the observed bipolar phenotype of cdk6-infected cells is especially interesting due to their similarity to glial progenitors. To further examine the role of cdk6 in these observed changes, the subcellular localization of cdk6 was studied.

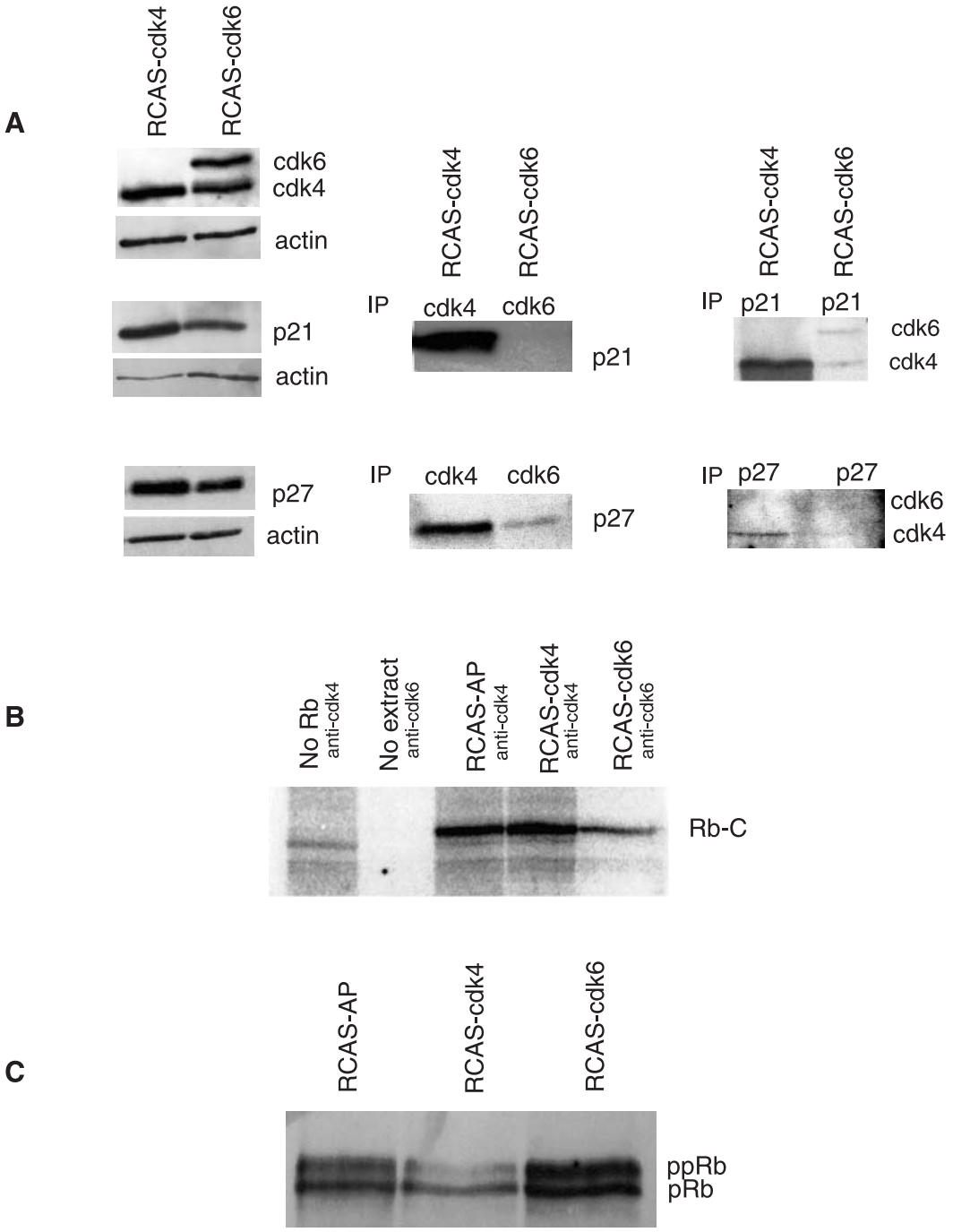

FIGURE 4. Binding assays and pRb kinase studies of cdk4- and cdk6-infected G-tva astroyctes. **A.** Immunoblots shown in the *left panels*. Amounts of protein loaded are as follows: cdk4/cdk6 blot, 125 μg; p21 blot, 100 μg; p27 blot, 150 μg. Cdk4/cdk6 immunoblot is probed with a mixture of both antibodies to allow visualization on the same blot. *Center panels* show cdk4 and cdk6 immunoprecipitations followed by immunoblot, as noted. *Right panels* show reciprocal immunoprecipitations followed by combined cdk4 and cdk6 immunoblot. All immunoprecipitations contained 750 μg of cell extract per lane. Assays are representative of at least two independent results. Actin immunoblots for loading controls are shown under each immunoblot. **B.** pRb kinase assay of AP-infected and cdk4-infected cells immunoprecipitated with antibody to cdk4- and cdk6-infected cells immunoprecipitated with antibody to cdk6. The two *left lanes* contain control reactions that lack Rb protein (*No Rb*) or a reaction with no added cell extract (*No extract*). **C.** pRb phosphorylation *in vivo*. Immunoblot of lysed cells. The positions of hypophosphorylated (*pRb*) and hyperphosphorylated (*ppRb*) are noted. Data are representative of at least two independent experiments.

Cdk4 and Cdk6 Are Differently Localized

Since p21 and p27 have been shown to direct cdk4 to the nucleus (39–41), and experiments shown in Fig. 4 indicated that cdk6 has a lower binding affinity than cdk4 for these proteins, indirect immunofluorescence was performed to examine the subcellular localization of cdk4 and cdk6. Previous studies have shown that cdk4 and cdk6 have distinct subcellular localizations in some cell types, with cdk6 staining

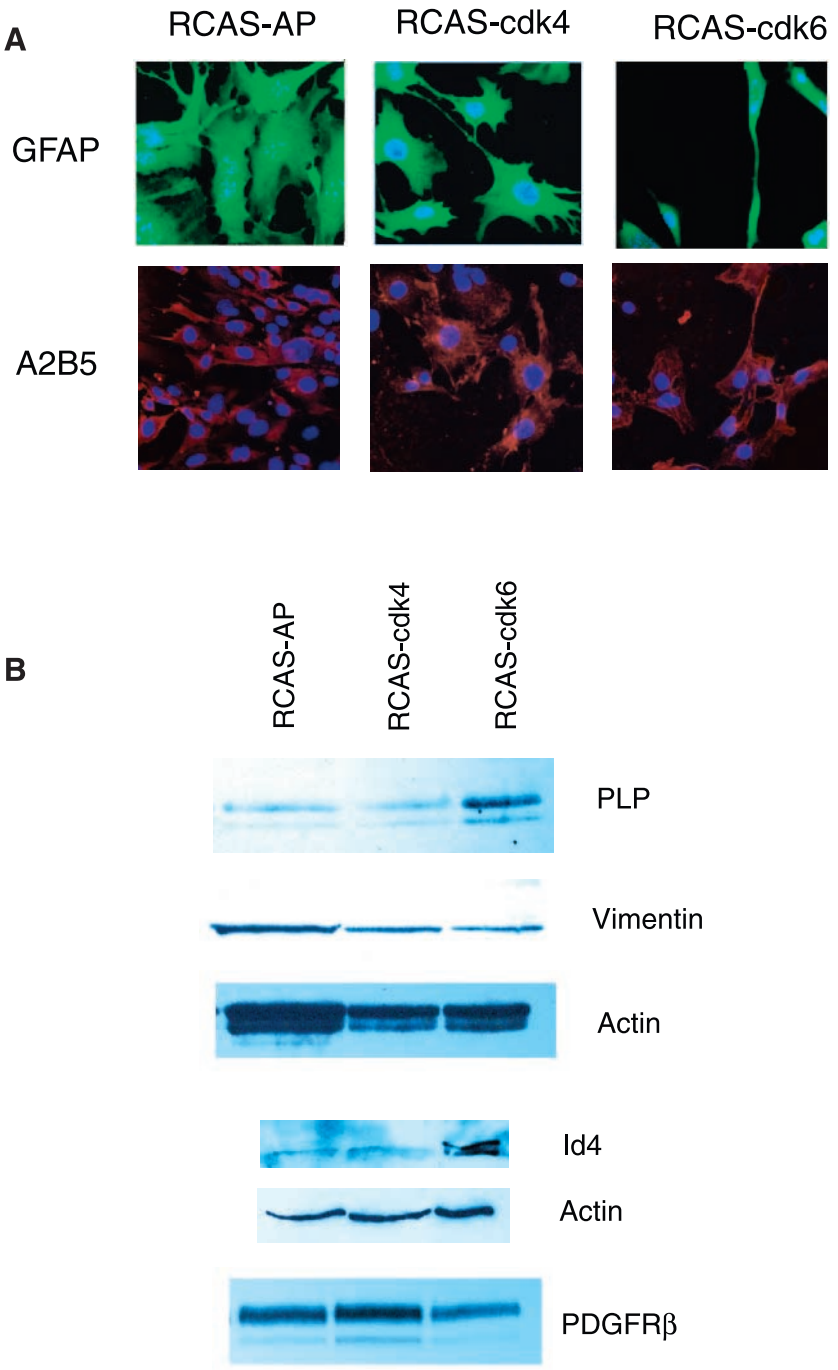

FIGURE 5. Expression of markers of differentiation in infected astrocytes. Immunofluorescence and immunoblots of known glial markers. **A.** Indirect immunofluorescence using GFAP (*green*) or A2B5 (*red*) as noted and counterstained with Hoechst (*blue*) to distinguish nuclei. **B.** Immunoblots of infected astrocytes probed with indicated antibody. Sizes are as follows: PLP, 30 kDa; Id4, 20 kDa; Vimentin, 50 kDa; PDGFRβ, 190 kDa. Blots shown are representative of at least three independent experiments and actin is blotted as a loading control. For immunoblots shown: blot of PLP/Vimentin contains 200 μg cell extract per lane; Id4, 100 μg per lane; and PDGFRβ, 25 μg cell extract loaded per lane.

heavily in the cytoplasm of some cells (9–11). Indirect immunofluorescence of cdk4 and cdk6 cells is shown in Fig. 6A along with its corresponding phase-contrast image and with a control of the same experimental procedure of fixed cells performed without incubation in primary antibody. Consistent with its decreased affinity for p21 and p27, these data clearly demonstrate that the cdk6 protein localizes heavily in the cytoplasm while cdk4 appears to stain more heavily in the nucleus. Cdk6 protein was localized throughout the cell including the long projections extending from the cell body and within bulbs that protrude from these projections. However, these studies make it difficult to determine if cdk6 is staining in the nucleus, or if the cytoplasm is overlaying the nucleus to generate the appearance of cdk6 nuclear staining. To distinguish between these two possibilities, immunofluorescence of paraformaldehyde-fixed monolayer cells was performed and cells were observed using confocal microscopy (Fig. 6B). In addition to extensive cytoplasmic staining, nuclear staining of cdk6 is clearly distinguished. These immunofluorescence studies clearly indicate that cdk6 is

localized to both the nucleus and to the cytoplasm while cdk4 kinase resides largely in the nucleus. These data again highlight important differences between the D-cyclin kinases cdk4 and cdk6. Differences in subcellular localization may be indicative of differences in the mechanism of action of these two kinases, including regulation of kinase activity, temporal timing of kinase activity, and/or a unique cytoplasmic role or substrate for cdk6.

Discussion

In this study, we have demonstrated that cdk4 and cdk6 have non-redundant functions in these primary mouse astrocytes. Primary mouse astrocytes were chosen as a model system because they contain minimal genetic mutations and provide a physiologically relevant system for the study of cancer. Gliomas comprise more than half of all primary brain tumors (38), and both cdk4 and cdk6 have been found to be overexpressed in these tumors (27–30). Interestingly, in one study, cdk6 expression was increased in 12 of 14 glioblastomas; however, it was not detected in any of the (14) lower grade matched tumor samples from the same patients (29). These data suggest that overexpression of cdk6 is a late event in astrocytic tumorigenesis. Data shown here highlight functional differences between cdk4 and cdk6.

In these studies, cdk6 expression resulted in a striking change in cellular morphology. These tissue-culture astrocytes did not express detectable levels of endogenous cdk6 before infection with virus containing the cdk6 cDNA. On infection of cdk6, but not its close homologue cdk4, cells underwent rapid morphogenesis that was consistently observed within the first days following infection. Cdk6 expression was both necessary and sufficient for this morphology change, since even when cdk4-infected astrocytes were super-infected with cdk6, the cells rapidly underwent this change to a bipolar morphology.

Reciprocal immunoprecipitations of infected astrocytes indicated that cdk4 has a higher affinity for p21 and p27 than does cdk6. These results are consistent with previous work in MEL cells which showed that pRB kinase activity of cdk4, but not cdk6, was inhibited in extracts overexpressing p27 and that p21 precipitated cdk2 and cdk4 but not cdk6 (24, 34, 35). It has been shown previously that p21 and p27 direct nuclear accumulation of cdk4 (39–41) and while several studies have localized cdk6 to the cytoplasm of a variety of cells, a correlation with Cip/Kip binding has not been made in these studies (9–11). Interestingly, indirect immunofluorescence in these astrocytes demonstrated that cdk6 was localized more heavily in the cytoplasm than was cdk4. This difference in subcellular localization between cdk4 and cdk6 correlates with differences in affinity of these kinases for p21 and p27. Since

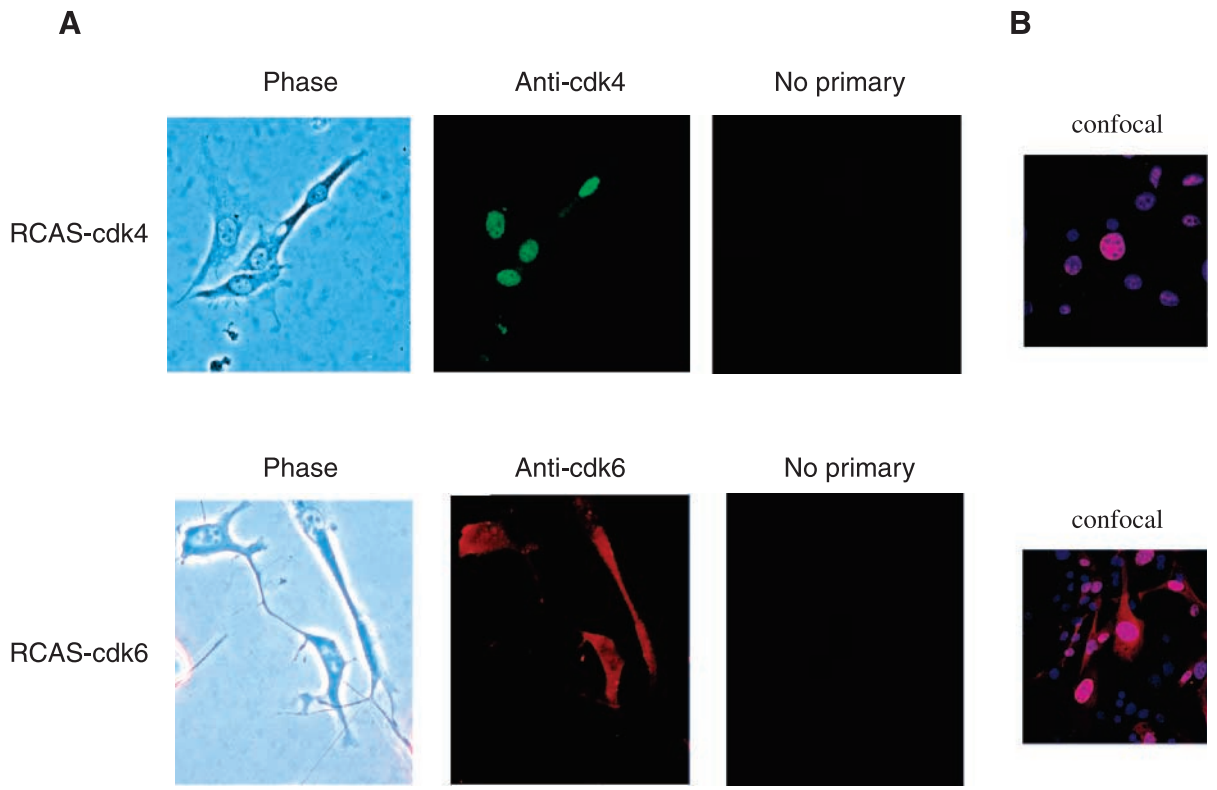

FIGURE 6. Subcellular localization of cdk4 and cdk6. Immunofluorescence of cdk4- and cdk6-infected astrocytes. **A.** Phase-contrast (*left panel*) and corresponding immunofluorescence images (*center panel*) are shown with a control (*right panel*) which was processed without any primary antibody. Cdk4 (*green*) shows strong nuclear staining while cdk6 (*red*) localizes heavily throughout the cell. **B.** Confocal microscopy of infected astroyctes showing cdk4 (*red*) and cdk6 (*red*) counterstained with DAPI stain (*blue*) to differentiate the nuclei. Results are representative of at least three independent experiments.

in vitro RB kinase activity is predominately derived from nuclear cdk6 (11, 24), and because the majority of cdk6 is located in the cytoplasm in some cell types (11), it is intriguing to speculate that cdk6 has a unique cytoplasmic substrate or function. While a cytoplasmic substrate of cdk6 has been previously identified (10), this substrate was also phosphorylated by cdk4.

The process of differentiation includes exit from the cell cycle followed by activation of tissue-specific genes (18). Some have proposed that an intrinsic timing mechanism causes withdrawal from the cell cycle and that this "timer" is triggered by the accumulation of inhibitory proteins, possibly in conjunction with the decay of stimulatory proteins (19–21). The cell cycle inhibitors p27 and p21 are likely one element of this timer. For instance, expression of p27 in early G_1 phase limits cdk2 activity, allowing differentiation of erythroid cells (34) and high levels of p27 protein are associated with differentiation of oligodendrocytes (19, 36). Expression of p21 has been associated with differentiation of keratinocytes (25, 26), muscle (22, 23), and MEL cells (24). Thus, up-regulation of the Cip/Kip inhibitors p21 and p27 is one mechanism by which cell cycle withdrawal occurs. The p21 and p27 proteins are known to act on both the D-cyclin kinase complexes and the cyclin E/cdk2 complex, although they may differ in their capacity to activate or inhibit these complexes. p21 and p27 have been shown to enhance the assembly of Cyclin D/cdk4 complexes and may result in activation of these kinases (39, 40, 42). In addition, certain complexes may have different affinities for these Cip/Kip proteins. For instance, cdk6-Cyclin D3 complex reportedly evades inhibition by p21 and p27 in arrested fibroblasts (43). Our data indicate that p27 and p21 bind cdk4 far better than cdk6 in immunoprecipitations from these infected astrocytes. Interestingly, a highly specific and ordered inhibition of the G_1 kinases may be required for differentiation in MEL cells: Inhibitors that blocked the combination of cdk6 and cdk2, but not cdk4 and cdk2, induced differentiation (24). Down-regulation of cdk6 activity was also implicated in another study of blood cell differentiation. Cdk6 protein levels and its associated *in vitro* pRB kinase activity decreased on induction of erythroid differentiation (34). We investigated the requirement for cdk6 kinase activity in morphology change by infecting astrocytes with a kinase-inactive mutant of cdk6, cdk6NFG (44). Several attempts to establish infections resulted in cell death of the viral producer cells and astrocytes, suggesting that these cells cannot tolerate this dominant-negative form of cdk6. This result warrants further investigation into the requirement for enzymatic activity of cdk6 in the morphological changes and associated changes in expression of markers of differentiation.

Data presented here indicate that cdk4 and cdk6 indeed have several non-overlapping functions including a role for cdk6 in morphological change and an association of cdk6 expression and the immature glial cell phenotype. Because cdk6 is a known cell cycle regulator that has been localized to the cytoplasm of several cell types, and because its expression results in a morphological change in astrocytes, cdk6 could provide both the cell cycle regulation and the cytoskeletal rearrangement required in the process of differentiation.

Materials and Methods

Construction of Plasmids and Vectors

RCAS-AP and RCAS-cdk4 were a kind gift of Eric Holland and have been previously described (31, 32). The human cdk6 cDNA was subcloned into plasmid pYI that contains an IRES and the GFP cDNA. From this subclone, the coding sequence for cdk6, IRES, and GFP was excised and inserted into RCAS-Y using *Not*I and *Pme*I sites in both vectors. Expression of cdk6 was confirmed by immunoblot and GFP expression of cdk6-infected cells was confirmed by fluorescence microscopy. The RCAS-cdk4 vector did not contain GFP coding sequences.

Infection of Primary Mouse Astrocytes and Growth Curves

DF-1 cells are chicken cells that produce the retrovirus on transfection with the RCAS plasmids. DF-1 cells were grown to 50% confluence in DMEM with 10% fetal bovine serum (FBS) and Penicillin/Streptomycin (Pen/Strep) (Cellgro, Herndon, VA) and transfected with 10 μg of RCAS plasmid and 10 μg carrier DNA by calcium phosphate precipitation (45). Immunoblots confirmed expression of AP, cdk4, or cdk6 protein in DF-1 cells. Virus-containing supernatants were harvested and passed through a 0.45-μm syringe filter onto 1×10^5 primary mouse astrocytes isolated from newborn G-tva chimeric mice (a kind gift of Eric Holland). Cells were infected for 3 or for 4 days with virus-containing supernatant that was changed twice and then carried in DMEM with 10% FBS and Pen/Strep. Confluent cells were removed by trypsin, counted, and replated at a density of 1×10^5 cells per 60-mm dish to generate growth curves.

Immunoblots and Immunoprecipitations

Cells were scraped from culture plates and collected in cold Dulbecco's PBS (JRH Biosciences, Lenexa, KS). Cells were resuspended in E1A Lysis Buffer (ELB) (250 mM NaCl, 50 mM Hepes, 5 mM EDTA, 0.1% NP40), with DTT, phenylmethylsulfonyl fluoride, leupeptin, and aprotinin. Cells were centrifuged at 16,000 × *g* for 20 min, supernatants were removed, and protein concentration was determined by protein assay (Bio-Rad, Hercules, CA). Extracts were used immediately or stored at −20°C. For immunoblots, 20–200 μg of protein extract (per lane, as noted) were analyzed by SDS-PAGE and transferred to supported nitrocellulose (Schleicher & Schuell, Keene, NH). After blocking in PBS containing 5% nonfat dry milk, blots were incubated with primary antibodies (Cdk4, cdk6, p16, and Id4: Santa Cruz Biotechnologies, Santa Cruz, CA; p15, p18, and actin: neoMarkers, Fremont, CA; p53: Oncogene Research Products, Cambridge, MA; p21 and p27: Becton Dickinson Co., San Jose, CA; pRb: PharMingen, San Diego, CA; PLP, vimentin: Chemicon, Temecula, CA; PDGFRβ: Upstate Biotechnology, Lake Placid, NY). Secondary antibodies used were anti-rabbit, anti-goat, or anti-mouse conjugated to horseradish peroxidase (Jackson Immunoresearch, West Grove, PA). Protein bands were visualized using enhanced chemiluminescence system (ECL) (Perkin-Elmer Life Sciences, Boston, MA).

For immunoprecipitations, 750–1000 μg cell extract (as noted) were incubated with 10 μl of indicated antibody. Cell

extracts and antibodies were incubated at 4°C for 60 min with rocking. Protein A-Sepharose CL-4B or Protein G-Sepharose 4 fastflow (Amersham Pharmacia Biotech, Piscataway, NJ) was added and extracts were rocked for 60 min to overnight at 4°C. Extracts and beads were centrifuged for 30 s at 200 × *g*, washed twice for 1 min in ELB without protease inhibitors, and resuspended in 40 μl 6 × SDS loading buffer, boiled, and loaded. Samples were separated by electrophoresis, transferred, and analyzed by immunoblot as described above. To assess p53-mediated DNA damage response, camptothecin (Sigma, St. Louis, MO) was added to cells at a concentration of 300 nM in DMSO for 24 h. Cells were extracted as above and 100 μg of cell extract was separated by SDS-PAGE, transferred to nitrocellulose, and probed with p21 antibody.

Scanning Electron Microscopy

Astrocytes were grown in Lab-Tek II two-chambered permanox slides (Nalge Nunc International, Naperville, IL) containing DMEM with 10% FBS and Pen/Step and incubated at 37°C for 48 h. Cells were fixed for 15 min in a modified Karnovsky's fixative containing 2% paraformaldehyde and 2.5% glutaraldehyde in 0.1 M phosphate buffer (pH 7.2) (46) and washed three times for 5 min in phosphate buffer. Cells were then fixed in 1% osmium tetroxide in 0.1 M phosphate buffer (pH 7.2) for 30 min followed by three washes of 2 min each in dH_2O. Cells were dehydrated at 4°C in a graded series of ethanol from 20% to 100% (46). After dehydration to 100%, cells were dried using a critical point drier. The permanox slides were cut into two squares of 20 mm × 20 mm and mounted on SEM supports using carbon tape. The dried cells were then sputter coated with gold–palladium for 70 s. Cells were examined on the SEM at 20 kV, beam current 200 μA, working distance 7 mm (47).

Immunofluorescence

Infected astrocytes were plated onto coverslips that had been preincubated in calf serum and then were grown until 50–70% confluent. Coverslips were washed twice in PBS and fixed in 4% paraformaldehyde at room temperature for 10 min. Coverslips were then processed or stored at −20°C. Coverslips were permeabilized in 95% ethanol, 5% acetic acid for 10 min at RT, washed three times in PBS containing 0.1% Tween (PBST), and incubated in 0.1 M glycine for 30 min at RT to decrease autofluorescence. Coverslips were blocked at RT for 30 min in PBST containing 10% serum (matching the source of secondary antibody). Cells were incubated in primary antibody for 60 min at RT in PBST containing 1% serum. Antibody sources were (cdk6, cdk4: Santa Cruz Biotechnologies; O4, GFAP, A2B5: Chemicon). Coverslips were washed three times in PBST and incubated in secondary antibody for 30 min at RT with Hoechst to stain DNA and differentiate nuclei. All secondary antibodies were supplied by Jackson Immunoresearch. Coverslips were mounted in Prolong (Molecular Probes, Eugene, OR) and examined using a Zeiss axioskop with digital imaging. Samples for confocal microscopy were seeded onto two-chambered slides and grown until near confluent. Cells were fixed in 4% paraformaldehyde and incubated in 0.1 M glycine as previously described. Cells were blocked in 10% FBS, 1% goat serum, and 0.1% saponin, and incubated with cdk4 or cdk6 primary antibodies as described. Anti-rabbit secondary fused to Alexa568 fluorochrome (Molecular Probes) was used with DAPI as a counterstain for DNA.

Kinase Assays and pRb Phosphorylation

Cells were scraped from culture plates with D-IP kinase buffer [50 mM Hepes (pH 7.5), 150 mM NaCl, 1 mM EDTA, 2.5 mM EGTA, 0.1% Tween 20, 10% glycerol] with protease inhibitors as noted above and phosphatase inhibitors as follows: 1 mM sodium fluoride, 0.1 mM sodium orthovanadate, and 1 mM β-glycerophosphate, final concentrations. Cells were sonicated twice for 10 s each and centrifuged to clear the lysate. Immunoprecipitations were performed with 1000 μg of cell extract and 10 μg of cdk4 (C-22) or cdk6 (C-21) (both Santa Cruz Biotechnologies) antibody as indicated for 4 h at 4°C with rocking. Protein A-Sepharose CL-4B was added and extracts were rocked 2 h at 4°C and then centrifuged for 30 s at 200 × *g*. Agarose pellets were washed three times in D-IP kinase buffer without protease inhibitors and twice in kinase reaction buffer [50 mM Hepes (pH 7.5), 10 mM $MgCl_2$, 2.5 mM EGTA, 1 mM DTT with protease and phosphatase inhibitors as above]. Kinase reactions included 25 μl kinase reaction buffer, 2 μg COOH-terminal pRb (QED Bioscience, San Diego, CA), 20 μM ATP, and 10 μCi γ^{32}P ATP. Reactions were incubated for 25 min at 30°C, stopped by the addition of 15 μl loading dye, and loaded onto a 10% polyacrylamide gel. Signals were detected using a Molecular Dynamics phosphorimager. This same extraction procedure was used for pRb phosphorylation analysis by immunoblot.

Acknowledgments

We thank Karl Münger and Jeffrey Singer for critical review of the manuscript and Eric Holland for the kind gift of astrocytes and vectors.

References

1. Elkholm, S. and Reed, S. Regulation of G1 cyclin-dependent kinases in the mammalian cell cycle. Curr. Opin. Cell Biol., *12:* 676–684, 2000.

2. Meyerson, M., Enders, G., Wu, C., Su, L., Gorka, C., Nelson, C., Harlow, E., and Tsai, L. A family of human cdc2-related protein kinases. EMBO J., *11:* 2909–2917, 1992.

3. Meyerson, M. and Harlow, E. Identification of G1 kinase activity for cdk6, a novel cyclin D partner. Mol. Cell. Biol., *14:* 2077–2086, 1994.

4. Matsushime, H., Ewen, M., Strom, D., Kato, J., Hanks, S., Roussel, M., and Sherr, C. Identification and properties of an atypical catalytic subunit (p34PSK-J3/cdk4) for mammalian D Type G1 cyclins. Cell, *71:* 323–334, 1992.

5. Matsushime, H., Quelle, D. E., Shurtleff, S. A., Shibuya, M., Sherr, C. J., and Kato, J. D-type cyclin-dependent kinase activity in mammalian cells. Mol. Cell. Biol., *14:* 2066–2076, 1994.

6. Nagasawa, M., Gelfand, E., and Lucas, J. Accumulation of high levels of the p53 and p130 growth-suppressing proteins in cell lines stably over-expressing cyclin-dependent kinase 6 (cdk6). Oncogene, *20:* 2889–2899, 2001.

7. Lucas, J., Terada, N., Szepsi, A., and Gelfand, E. Regulation of synthesis of p34cdc2 and its homologues and their relationship to p110Rb phosphorylation during cell cycle progression of normal human T cells. J. Immunol., *148:* 1804–1811, 1992.

8. Lucas, J., Terada, N., Szepsi, A. and Gelfand, E. Differential regulation of the synthesis and activity of the major cyclin-dependent kinases, p34cdc2, p33cdk2, and p34cdk4, during cell cycle entry and progression in normal human T lymphocytes. J. Cell. Physiol., *165:* 406–416, 1995.

9. Fahraeus, R. and Lane, D. The p16INK4a tumour suppressor protein inhibits αvβ3 integrin-mediated cell spreading on vitronectin by blocking PKC-dependent localization of αvβ3 to focal contacts. EMBO J., *18:* 2106–2118, 1999.

10. Kwon, T., Buchholz, M., Gabrielson, E., and Nordin, A. A novel cytoplasmic substrate for cdk4 and cdk6 in normal and malignant cells. Oncogene, *11:* 2077–2083, 1995.

11. Mahony, D., Parry, K., and Lees, E. Active cdk6 complexes are predominantly nuclear and represent only a minority of the cdk6 in T cells. Oncogene, *16:* 603–611, 1998.

12. Nagasawa, M., Melamed, I., Kupfer, A., Gelfand, E., and Lucas, J. Rapid nuclear translocation and increased activity of cyclin-dependent kinase 6 after T cell activation. J. Immunol., *158:* 5146–5154, 1997.

13. Wolfel, J., Hauer, M., Schneider, J., Serrano, M., Wolfel, C., Klehmann-Hieb, E., De Plaen, E., Hankelen, T., Meyer zum Buschenfelde, K., and Beach, D. A p16 INK4a-insensitive CDK4 mutant targeted by cytolitic T lymphocytes in a human melanoma. Science, *269:* 1281–1284, 1995.

14. Zuo, L., Weger, J., Yang, Q., Goldstein, A., Tucker, M., Walker, G., Hayward, N., and Dracopoli, N. Germline mutations in the p16INK4a binding domain of CDK4 in familial melanoma. Nat. Genet., *12:* 97–99, 1996.

15. Piboonniyom, S., Timmermann, S., Hinds, P., and Münger, K. Aberrations in the MTS1 tumor suppressor locus in oral squamous cell carcinoma lines preferentially affect the *INK4A* gene and result in increased cdk6 activity. Oral Oncol., *38:* 179–186, 2002.

16. Timmermann, S., Hinds, P. W., and Munger, K. Elevated activity of cyclin-dependent kinase 6 in human squamous cell carcinoma lines. Cell Growth & Differ., *8:* 361–370, 1997.

17. Easton, J., Wei, T., Lahti, J., and Kidd, V. Disruption of the cyclin D/cyclin-dependent Kinase/INK4/retinoblastoma protein regulatory pathway in human neuroblastoma. Cancer Res., *58:* 2624–2632, 1998.

18. Yee, A., Shih, H., and Tevosian, S. New perspectives on retinoblastoma family functions in differentiation. Front. Biosci., *3:* d532–d547, 1998.

19. Casaccia-Bonnefil, P., Tikoo, R., Kiyokawa, H., Friedrich, V., Chao, M., and Koff, A. Oligodendrocyte precursor differentiation is perturbed in the absence of the cyclin-dependent kinase inhibitor p27Kip1. Genes Dev., *11:* 2335–2346, 1997.

20. Durrand, B., Fero, M., Roberts, J., and Raff, M. p27Kip1 alters the response of cells to mitogen and is part of a cell-intrinsic timer that arrests the cell cycle and initiates differentiation. Curr. Biol., *8:* 431–440, 1998.

21. Tikoo, R., Casaccia-Bonnefil, P., Chao, M., and Koff, A. Changes in cyclin-dependent kinase 2 and p27kip1 accompany glial cell differentiation of central Glia-4 cells. J. Biol. Chem., *272:* 442–447, 1997.

22. Parker, S., Eichele, G., Zhang, P., Rawls, A., Sands, A., Bradley, A., Olson, E., Harper, W., and Elledge, S. p53-Independent expression of p21Cip1 in muscle and other terminally differentiating cells. Science, *267:* 1024–1027, 1995.

23. Skapek, S., Rhee, J., Spicer, D., and Lassar, A. Inhibition of myogenic differentiation in proliferating myoblasts by cyclin D1-dependent kinase. Science, *267:* 1022–1024, 1995.

24. Matushansky, I., Radparvar, F., and Skoultchi, A. Reprogramming leukemic cells to terminal differentiation by inhibiting specific cyclin-dependent kinases in G1. Proc. Natl. Acad. Sci., *97:* 14317–14322, 2000.

25. DiCunto, F., Topley, G., Calautti, E., Hsiao, J., Ong, L., Seth, P., and Dotto, P. Inhibitory function of p21 cip1/WAF1 in differentiation of primary mouse keratinocytes independent of cell cycle control. Science, *280:* 1069–1072, 1998.

26. Missero, C., DiCunto, F., Kiyokawa, H., Koff, A., and Dotto, G. The absence of p21Cip1/Waf1 alters keratinocytes growth and differentiation and promotes *ras*-tumor progression. Genes Dev., *10:* 3065–3075, 1996.

27. Costello, J. F., Plass, C., Arap, W., Chapman, V. M., Held, W. A., Berger, M. S., Huang, H. S., and Cavanee, W. K. Cyclin-dependent kinase 6 (cdk6) amplification in human gliomas identified using two-dimensional separation of genomic DNA. Cancer Res., *57:* 1250–1254, 1997.

28. Ichimura, K., Schmidt, E., Goike, H., and Collins, V. P. Human glioblastomas with no alterations of the CDKN2A (p16INK4A, MTS1) and CDK4 genes have frequent mutations of the retinoblastoma gene. Oncogene, *13:* 1996.

29. Lam, P., Ditamaso, E., Ng, H., Pang, J., Roussel, M., and Hjelm, N. Expression of p19INK4d, cdk4, cdk6 in glioblastoma multiforme. Br. J. Neurosurg., *14:* 28–32, 2000.

30. Schmidt, E., Ichimura, K., Reifenberger, G., and Collins, P. CDKN2 (p16/MTS1) gene deletion or CDK4 amplification occurs in the majority of gliobastomas. Cancer Res., *54:* 6321–6324, 1994.

31. Holland, E. C. and Varmus, H. E. Basic fibroblast growth factor induces cell migration and proliferation after glia-specific gene transfer in mice. Proc. Natl. Acad. Sci., *95:* 1218–1223, 1998.

32. Holland, E. C., Hively, W. P., Gallo, V., and Varmus, H. E. Modeling mutations in the G1 arrest pathway in human gliomas: overexpression of cdk4 but not loss of INK4a-ARF induces hyperploidy in cultured mouse astrocytes. Genes Dev., *12:* 3644–3649, 1998.

33. Lee, J., Mayer-Proschel, M., and Rao, M. Gliogenesis in the central nervous system. Glia, *30:* 105–121, 2000.

34. Hsieh, F., Barnett, L., Green, W., Freedman, K., Matushansky, I., Skoultchi, A., and Kelley, L. Cell cycle exit during terminal erythroid differentiation is associated with accumulation of p27kip1 and inactivation of cdk2 kinase. Hematopoiesis, *96:* 2746–2754, 2000.

35. Matushansky, I., Radparvar, F., and Skoultchi, A. Manipulating the onset of cell cycle withdrawal in differentiated erythroid cells with cyclin-dependent kinases and inhibitors. Hematopoiesis, *96:* 2755–2764, 2000.

36. Kondo, T. and Raff, M. The Id4 HLH protein and the timing of oligodendrocyte differentiation. EMBO J., *19:* 1998–2007, 2000.

37. Rao, M., Noble, M., and Mayer-Pröschel, M. A tripotential glial precursor cell is present in the developing spinal cord. Proc. Natl. Acad. Sci. USA, *95:* 3996–4001, 1998.

38. Dai, C., Celestino, J., Okada, Y., Louis, D., Fuller, G., and Holland, E. PDGF autocrine stimulation dedifferentiates cultured astrocytes and induces oligodendrogliomas and oligoastrocytomas from neural prgenitors and astrocytes *in vivo*. Genes Dev., *15:* 1913–1925, 2001.

39. LaBaer, J., Garrett, M. D., Stevenson, L. F., Slingerland, J. M., Sandhu, C., Chou, H. S., Fattaey, A., and Harlow, E. New functional activities for the p21 family of CDK inhibitors. Genes Dev., *11:* 847–862, 1997.

40. Reynisdottir, I. and Massague, J. The subcellular locations of p15ink4b and p27kip1 coordinate their inhibitory interactions with cdk4 and cdk2. Genes Dev., *11:* 492–503, 1997.

41. Diehl, A. and Sherr, C. A dominant-negative cyclin D1 mutant prevents nuclear import of cyclin-dependent kinase 4 (cdk4) and its phosphorylation by CDK-activating kinase. Mol. Cell. Biol., *17:* 7362–7374, 1997.

42. Cheng, M., Olivier, P., Diehl, A., Roberts, J., and Sherr, C. The p21 cip1 and p27 kip1 CDK 'inhibitors' are essential activators of cyclin D-dependent kinases in murine fibroblasts. EMBO J., *18:* 1571–1583, 1999.

43. Lin, J., Jinno, S., and Okayama, H. Cdk6-cyclin D3 complex evades inhibition by inhibitor proteins and uniquely controls cell's proliferation competence. Oncogene, *20:* 2000–2009, 2001.

44. van den Heuvel, S. and Harlow, E. Distinct roles for cyclin-dependent kinases in cell cycle control. Science, *262:* 2050–2054, 1993.

45. Chen, C. and Okayama, H. High-efficiency transformation of mammalian cells by plasmid DNA. Mol. Cell. Biol., *7:* 2745–2752, 1987.

46. Bozzola, J. and Russel, L. Electron Microscopy. Sudbury, MA: Jones and Bartlett Publishers, Inc., 1999.

47. Allen, T. The application of scanning electron microscopy to cells in culture: selected methodologies. *In:* Scanning Electron Microscopy IV, pp. 1963–1972. Chicago: Jones and Bartlett, 1983.

Molecular Cancer Research

Expression of Cyclin-Dependent Kinase 6, but not Cyclin-Dependent Kinase 4, Alters Morphology of Cultured Mouse Astrocytes[1]1NSF under CAREER grant #9984454 to Martha J. Grossel.

Karen K. Ericson, David Krull, Peter Slomiany, et al.

Mol Cancer Res 2003;1:654-664.